Journal of the Optical Society of America B
OPTICAL PHYSICS

Toward ultimate nanophotonic light trapping using pattern-designed quasi-guided mode excitations

YAN-KAI ZHONG, SZE-MING FU, NYAN PING JU, AND ALBERT LIN*

Department of Electronic Engineering, National Chiao-Tung University, Hsinchu 30010, Taiwan
**Corresponding author: hdtd5746@gmail.com*

Received 26 March 2015; revised 7 May 2015; accepted 7 May 2015; posted 7 May 2015 (Doc. ID 236839); published 1 June 2015

In this work, a shape-optimized periodic pattern design is employed to boost the short circuit current of solar cells. A decent result of an additional 16.1% enhancement in short circuit current is achieved by solely pattern-wise optimization, compared to the baseline structure that is already under full parameter optimization. The underlying physics is that the shape-optimized pattern leads to optimal quasi-guided mode excitations. As a result of the pattern design, a single strongly confined quasi-guided mode is replaced with several weakly confined modes, to cover a broader spectral range. Previous works of optimized periodic gratings result in gradually varied grating heights and require grayscale lithography leading to high process complexity. Using randomized pattern for isotropic Lambertian light trapping, on the other hand, leads to an overly large simulation domain. The proposed pattern design methodology achieves the optimal balance between the slow-light enhancement strength and the enhancement spectral range for nanophotonic light trapping using quasi-guided modes.

OCIS codes: (310.6845) Thin film devices and applications; (050.1940) Diffraction; (040.5350) Photovoltaic.

http://dx.doi.org/10.1364/JOSAB.32.001252

1. INTRODUCTION

The randomly textured surface [1,2] has been used for a long time because of its isotropic Lambertian emission. The well-known drawback for randomized structure is the difficulty in simulation and optimization because of its overly large dimension. Although there is some effort on the design and the optimization of randomized structures, it is pretty much limited to the quasi-random scenario [3–10] because of limited computational resources. Recent effort on the periodic grating for solar cells draws significant attention. The use of quasi-guided mode excitation via periodic grating couplers is a promising alternative to the randomized structures [11–24]. At the vicinity of the mode excitation wavelengths, the slow-light enhancement can be achieved. Thus, the photon group velocity (v_g) is reduced to extend the photon lifetime trapped inside the semiconductor active layer. Circularly shaped periodic gratings are employed in most cases. The grating couplers initiate strong light scattering and mode confinement, and efficient light trapping comparable to randomized structures is possible. The recent work by Battaglia *et al.* concludes that the periodic grating and randomized ones can achieve roughly the same level of nanophotonic light trapping [25]. From the viewpoint of design and optimization, it seems to us that the periodic structure is more promising than the randomized ones. This is primarily because of the fact that the randomized structures can lead to significant difficulty in the design. This is the reason why optimized fully randomized structure has not been realized to date.

The optimization of periodic structures has been initiated by several groups [4,26]. In these earlier works, promising improvement is achieved but the result can lead to the need for grayscale lithography or holographic lithography. This is because the proposed structures usually possess continuous height variation. To use regular simple lithography techniques, such as nanoimprint [16,17,25,27], the height variation of the periodic grating cannot be continuous. For example, a sinusoidal-depth-profile laminar grating requires grayscale lithography while a step-wise rectangular grating does not.

The requirement of using only step-wise gratings means that the optimization can only be in the "**shape**" of the etched pattern. This work shows that, by sole shape optimization using complex photonic pattern design, the effective photon lifetime and the effective material photonic density of state (PDOS) can still be increased significantly, which increases the solar cell efficiency. The fact that the shape-optimized periodic grating structures do not require grayscale or holographic lithography makes this proposal very practical. The fabrication complexity is not significantly increased, compared to a regular periodic grating in solar cells while the complexly designed photonic

pattern can further boost the optical absorbance by >16%. The proposed pattern design can be employed in any solar cell technologies using any material systems.

2. PROBLEM SETUP FOR PATTERN OPTIMIZATION

The pattern design is a complicated task. There are several different aspects to consider before decent slow-light resonance enhancement can be attained using periodic patterns. The first one is the feasibility of the patterns as far as the lithography process is concerned. Nanoimprint lithography is suitable for the photovoltaic application, since it is of low-cost and large-area nature [27]. The resulting optimized patterns should not be too fine to resolve and, therefore, the evolutionary scheme in global optimization requires some contemplation. The second important consideration is symmetry or a polarization-averaged absorption. Using a symmetric pattern makes the calculation simpler since the spectral response is the same for different polarizations. Using nonsymmetrical patterns, on the other hand, requires the calculation of a polarization averaged absorption to reflect the true light trapping capability of the structures.

This is illustrated in Fig. 1, where patterns with different degrees of symmetry are plotted. The dashed lines in Fig. 1 are the symmetry axes. Thus, the baseline circularly shaped grating in Fig. 1(a) is of > fourfold symmetry. In fact, it is isotropic, and the polarization independence of the incident light at least at normal incidence can be achieved easily. This can be verified by calculating the optical absorbance, i.e., short circuit current under perfect charge collection, for the normal incidence light of different polarizations. The pattern in Fig. 1(b) is of fourfold symmetry. Such a pattern has the same spectral response for *s*-, *p*-, and 45-degree polarizations, which is trivial by examining the symmetry. In fact, the spectral response is the same for Fig. 1(b) at all polarizations under normal incidence, even if the pattern itself is not totally isotropic.

The pattern in Fig. 1(c) has twofold symmetry. It is mirror-symmetric with respect to the *x*-axis and *y*-axis. The patterns that fall into this category include circularly shaped gratings in a hexagonal lattice. The pattern in Fig. 1(c) has different spectral responses for *s*- and *p*-polarized light under normal incidence conditions. The spectral response for the 45-degree polarization can be calculated as the average of the *s*- and *p*-polarizations. The spectral response of the other polarizations can be calculated as weighted averaged of *s*- and *p*-polarizations. Figure 1(d) is a pattern with only onefold symmetry. In this case, the spectral response for the 45-degree polarization is not the average of *s*- and *p*-polarizations, in general. The spectral response for any linearly polarized light can be calculated by knowing the 45-degree response first and using Eq. (3). For elliptically polarized light, the response for an arbitrary polarization can also be known by using Eq. (3) with the knowledge of the 45-degree and circular polarization responses. Figure 1(e) is a pattern without any symmetry axis. In this case, to have a fair judge on its light trapping capability, a polarization-averaged absorption has to be calculated.

After understanding the symmetry property and polarizations, we can proceed to the pattern optimization problem for solar cells. Given the fact that the solar illumination is polarized randomly, the pattern should be leading to high optical absorbance for all polarizations. There are two ways to achieve this. One is using a symmetric pattern such as Fig. 1(b) or 1(c). A test run on the pattern optimization using a twofold symmetry pattern has been conducted in our group. Nonetheless, it is found that the optimization is not efficient on boosting the absorbance. The procedure to construct a symmetric pattern is first defining a pattern in the first quadrant. Afterward, the pattern is replicated with mirror symmetry into the other quadrants. This results in smaller design or optimization space, and leads to lower enhancement from our test runs. A more elaborated pattern evolution scheme may be necessary to attain satisfactory results. We afterward transit to nonsymmetrical patterns, and to take into account the randomly polarized sunlight, the responses at all polarization angles are calculated using Eq. (3). The polarization averaged values are then used as the figure of merit during the global optimization. This is an alternative to the symmetric pattern methodology.

The calculation procedure is as follows: first, the spectral absorbance (A) is calculated for *s*-polarizations. This is done by integrating the power dissipation in the semiconductor:

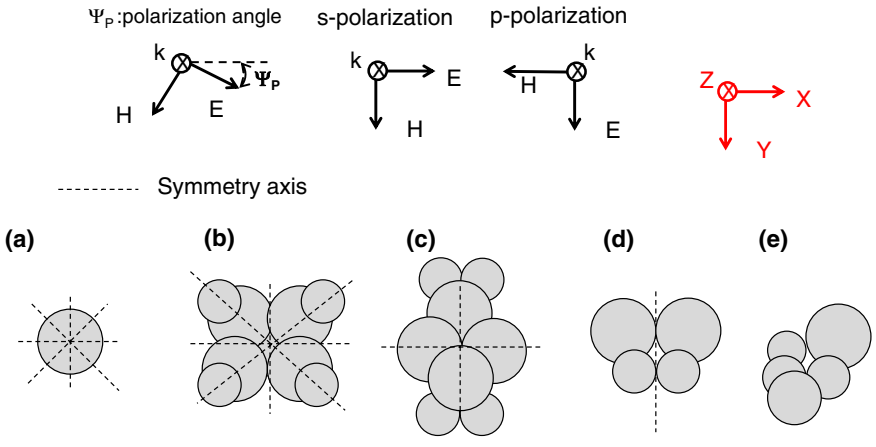

Fig. 1. Symmetry consideration for the patterns of solar cell grating design. (a) The pattern is isotropic in all directions. (b) The pattern has fourfold symmetry. (c) The pattern has twofold symmetry. (d) The pattern has onefold symmetry. (e) The pattern has no symmetry. Ψ_p is the polarization angle.

$$A_S(\lambda) = \frac{\frac{1}{2}\int_V \omega\varepsilon_0\varepsilon''(\lambda)|\vec{E}_S(\vec{r})|^2 \mathrm{d}v}{\frac{1}{2}\int_S \mathrm{Re}\{\vec{E}_S(\vec{r}) \times \vec{H}_S^*(\vec{r})\} \cdot \mathrm{d}\vec{S}}, \quad (1)$$

where ω is the angular frequency, λ is the free space wavelength, ε_0 is the permittivity in vacuum, and ε'' is the imaginary part of the complex semiconductor dielectric constant. A similar procedure is repeated for p- and 45-degree polarizations. It should be emphasized that, although the result here is for thin-film polycrystalline silicon photovoltaics, the proposed optimization scheme together with the pattern design methodology can fit easily into other solar cell technologies. An arbitrarily polarized incidence can actually be decomposed into s- and p-polarizations:

$$\begin{aligned}\vec{E}_{45,\mathrm{lin}} &= \frac{1}{\sqrt{2}}\vec{E}_S + \frac{1}{\sqrt{2}}\vec{E}_P,\\ \vec{E}_{\mathrm{cir}} &= \frac{1}{\sqrt{2}}\vec{E}_S + \frac{1}{\sqrt{2}}i\vec{E}_P\\ \vec{E}_{\Psi_p} &= a\vec{E}_S + b\vec{E}_P, \end{aligned} \quad (2)$$

where E is the incident electric field, and the subscript denotes s-, p-, 45-degree, circular, or arbitrary polarization. Ψ_P denotes an arbitrary polarization angle. For 45-degree and circularly polarized light, equal amounts of s- and p-polarized components exist.

It should be emphasized that, although the Eq. (2) indicates that any polarization can be decomposed linearly into s- and p-polarizations, this does not necessary mean that the optical absorbance can also be calculated as the linear superposition of s- and p-polarized responses. The power, i.e., Poynting vector, and the power absorption, i.e., Joule heating, are proportional to the square of the electric and magnetic field amplitudes; therefore, the cross terms exist. Simply averaging the absorption may lead to an incorrect result for many cases. The absorption at an arbitrary polarization angle Ψ_P can be calculated by

$$\begin{aligned}A_{\Psi_p}(\lambda) = &\frac{1}{a^2+b^2}\\ &\times [a^2A_S(\lambda) + b^2A_p(\lambda) + \mathrm{real}(a^*b)\\ &\times (2A_{45,\mathrm{lin}}(\lambda) - A_S(\lambda) - A_p(\lambda)) - \mathrm{imag}(a^*b)\\ &\times (2A_{\mathrm{cir}}(\lambda) - A_S(\lambda) - A_p(\lambda))]. \end{aligned} \quad (3)$$

a and b are defined in Eq. (2). A_s, A_p, $A_{45,\mathrm{lin}}$, and A_{cir} are the responses for s-polarization, p-polarization, 45-degree polarizations, and circular polarization. Ψ_P denotes an arbitrary polarization angle. If the fourfold or twofold symmetry stated in Fig. 1 exists, the 45-degree polarization response will be the average of s- and p-polarizations. In this case, Eq. (3) reduces to a simple weighted averaging formula. The last term involving the circularly polarized light will only be needed in the case of elliptically polarized light. The polarization averaged absorbance at a single wavelength is defined as

$$A_{\mathrm{avg}}(\lambda) = \int_{\Psi_p} A_{\Psi_p}(\lambda)\mathrm{d}\Psi_P. \quad (4)$$

The weighted, integrated absorbance (A_{Int}) over a broadband solar spectrum is defined as

$$A_{\mathrm{Int}} = \frac{\int \frac{\lambda}{hc}\Omega(\lambda)A_{\mathrm{avg}}(\lambda)\mathrm{d}\lambda}{\int \frac{\lambda}{hc}\Omega(\lambda)\mathrm{d}\lambda}, \quad (5)$$

where Ω is the AM1.5 solar spectrum. This definition is the same as the short circuit current (J_{SC}) under ideal charge collection if Ω is in the unit of $\#s^{-1}\,m^{-1}\,nm^{-1}$.

Thin-film polycrystalline silicon (poly-Si) solar cells are used as an example to demonstrate the effectiveness of the pattern-designed methodology. The material parameters are from the Rsoft material database [28]. Poly-silicon material parameters are from the SOPRA material database. The optimization result demonstrated by thin-film poly-Si is included in this paper. It should be emphasized that the proposed design not only works for silicon of different phases, but also can provide efficient nanophotonic light trapping for other inorganic semiconductors. This is because of the similar mode coupling, light trapping, and waveguiding behaviors in inorganic solar cells. One example is that the TiO_2 nanotips [12] are originally proposed based on simulation with silicon solar cells, but later it can be applied to III–V solar cells equally well [29]. As a result, the inorganic semiconductor that is used as an example here to demonstrate the effectiveness of pattern design and optimization is not critical. The calculation method is based on rigorously coupled wave analysis (RCWA) implemented by the Rsoft Diffractmode.

A genetic algorithm (GA) or evolutionary algorithm is a stochastic global search method that mimics the metaphor of natural biological evolution [30]. The principle of survival of the fittest is applied to a population of individuals, which are potential solutions to the problem. Individuals with higher fitness in the problem domain have a better chance to be selected and to reproduce their own offspring. Genetic algorithms are particularly suited for search in very large or unbounded sample spaces, and it has been proven useful in many different fields [31–34]. In the case of pattern design in solar cells, the complexity associated with the wave nature of light and broad solar spectrum results in a similar large sample space for possible grating structures for optimization of solar cell efficiency.

3. BASELINE DESIGN: THE PHOTONIC CIRCULARLY SHAPED GRATING UNDER FULL PARAMETER OPTIMIZATION

Figure 2 illustrates the baseline design using a circularly shaped grating. A polycrystalline silicon thickness (t_{PolySi}) of 200 nm is chosen to have a thinner solar cell to make the light trapping effect more pronounced. This practice can make the comparison of light trapping capability for various patterns more meaningful since, for thin solar cells, the light trapping effect is more dominant. Besides, reduced thickness photovoltaics is an important future direction for all solar cell technologies. Indium tin oxide (ITO) is used as transparent contacts, and a silver (Ag) back reflector is used. The circularly shaped photonic crystal has been commonly used in solar cell light trapping, either in theoretical or experimental effort. The baseline structure is illustrated in Fig. 2, where the circularly shaped grating is formed on the dielectric spacer. In this case, the altitude of the circular region is higher than the surrounding, i.e., the elevated circular region. To form the nanophotonic

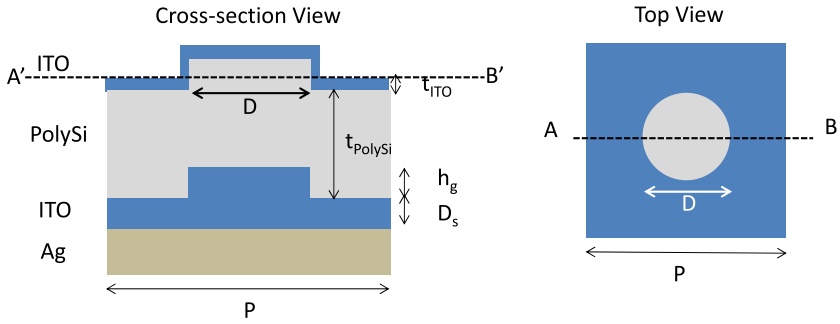

Fig. 2. Illustration of the baseline structure for the nanophotonic light trapping. The circularly shaped photonic crystal (PC) array is optimized in its parameters using a global optimization algorithm. The solar cell stack consists of indium tin oxide (ITO), polycrystalline silicon (poly-Si), indium tin oxide (ITO), and silver (Ag).

patterns on solar cell substrates, nanoimprint lithography (NIL) can be employed, since it has been proven to be a cost-effective method to form large-area solar cell light trapping patterns [27]. For the baseline devices, we want to calculate the integrated optical absorbance (A_{Int}) achievable by a periodic array of circular gratings, with solar cell geometry parameters fully optimized.

Figure 3 plots the spectral response for the baseline device with full parameter optimization. The geometry of the baseline devices is optimized by a genetic algorithm to locate the globally maximized optical absorbance for the baseline pattern. The optimized geometry is $P = 473$ nm, $t_{\mathrm{ITO}} = 55$ nm, $D = 366$ nm, $h_g = 142$ nm, and $D_{\mathrm{st}} = 212$ nm for the baseline structure illustrated in Fig. 2. The maximized integrated absorbance achieved is 0.573. The quasi-guided mode excitation above the light cone is the important underlying physics for the solar cell absorption enhancement using a periodic grating. Nonetheless, it will be clear that the fully optimized circularly shaped grating can be further improved. The improvement is through the shape optimization, which can provide additional efficiency enhancement without the need for grayscale or holographic lithography. The strong resonance

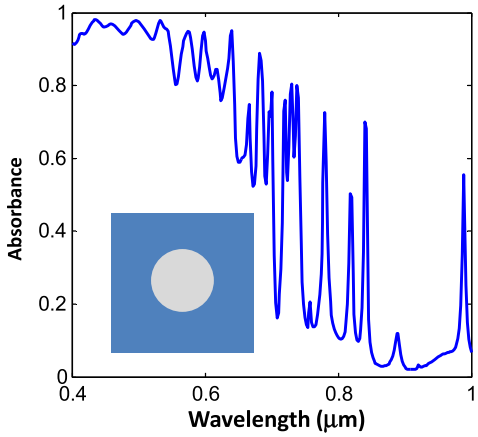

Fig. 3. Baseline spectral response for the circularly shaped grating array. The geometry is fully optimized by a genetic algorithm. Strongly confined modes at specific long wavelengths indicate the narrowband slow-light enhancement. Later it will be shown that further improvement can be done by breaking a single strong resonance into several weaker resonances to cover a broader spectral range.

peaks in the spectral response in Fig. 3 indicate strong mode confinement and very slow photon group velocity (v_g) at the excitation wavelengths. Nonetheless, the broadband enhancement may not be achieved optimally using narrowband strong confinement modes. To tailor the photonic band structure that, in turn, affects the photonic density of state (PDOS) and photon group velocity (v_g), the shape optimization scheme is employed below in Section 4.

4. PATTERN OPTIMIZATION FOR SHAPE-OPTIMIZED PERIODIC PATTERNS

Figure 4 illustrates the devices with complex photonic pattern designs. A polycrystalline silicon thickness (t_{Si}) of 200 nm is also chosen, as in the baseline devices in the previous section. The pattern design is achieved by adjusting the radius and the position of $N_C = 10$ circles, using a global optimization technique, in the solar cell structure. The superposition of circles forms the complex photonic pattern. The pattern design can be made even more elaborate if additional circles or geometrical elements are used when forming the complex photonic pattern. The absorbance is a polarization averaged value. In this case, the two-dimensional irregularly shaped silicon pillar array after optimization is not rotationally symmetric. As a result, *s*- and *p*-polarized light have different responses.

Figure 5 plots the spectral response and the field profiles in the case of the optimized device with a complex photonic pattern design. The geometry of the pattern-designed solar cell is optimized by a genetic algorithm, to locate the globally maximized topology for solar cell light trapping. The optimized geometry is $P = 576$ nm, $t_{\mathrm{ITO}} = 54$ nm, $D = 167$ nm, $h_g = 172$ nm, and $D_{\mathrm{st}} = 248$ nm for the structure illustrated in Fig. 4. The maximized integrated absorbance achieved is 0.665 for the pattern-designed structure, which is 16.1% higher than the baseline device in Section 3. In Fig. 5, the field plots at different wavelengths show the phenomena of photon in-coupling and quasi-guided mode excitations. From the profiles at short wavelengths, the high extinction coefficient results in fast decay of solar photons once they are coupled into the active absorbing layer. In this case, the purpose of the pattern design is to tailor the solar cell front surface to provide effective anti-reflection and photon in-coupling. In the case of long wavelengths, the quasi-guide modes are excited, which can be seen at $\lambda = 800$ nm and at $\lambda = 1000$ nm, where optical

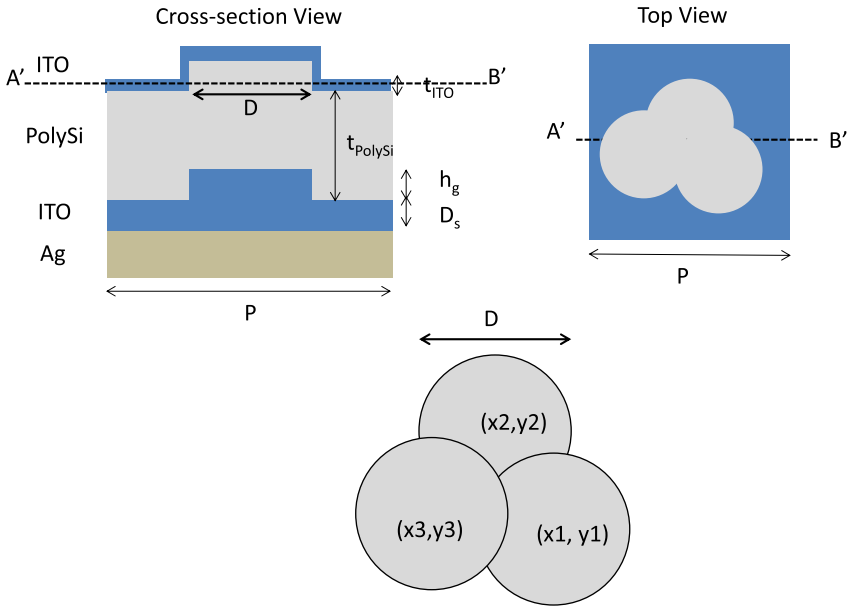

Fig. 4. Illustration of the photonic pattern-designed structures. The multiple circles are varied in their diameter and positions to form the complex photonic pattern. In the actual simulation, $N_C = 10$ circles are used to form the pattern. The fabrication-wise complexity is not significantly increased from the baseline structure, as illustrated in Fig. 2. The shape-optimization of the periodic grating pattern is effective in tailoring the photonic band structure. The slow-light enhancement spectral range and mode confinement factor are determined by the slope of the photonic band structure ω-k. Using shape optimization is more feasible than other methods that may require grayscale or holographic lithography. The solar cell stack consists of indium tin oxide (ITO), polycrystalline silicon (poly-Si), indium tin oxide (ITO), and silver (Ag).

modes are confined in the poly-Si layer. In this scenario, the photons are propagating in the in-plane direction of the poly-Si layer, and the solar cell stack acts effectively as a waveguide to provide slow-light enhancement.

The solar cell broadband light trapping not only needs the strong resonance at specific wavelengths, but also a broadband compromise. The shape optimization generally self-adjusts the photonic pattern to better fit the purpose of solar cell light

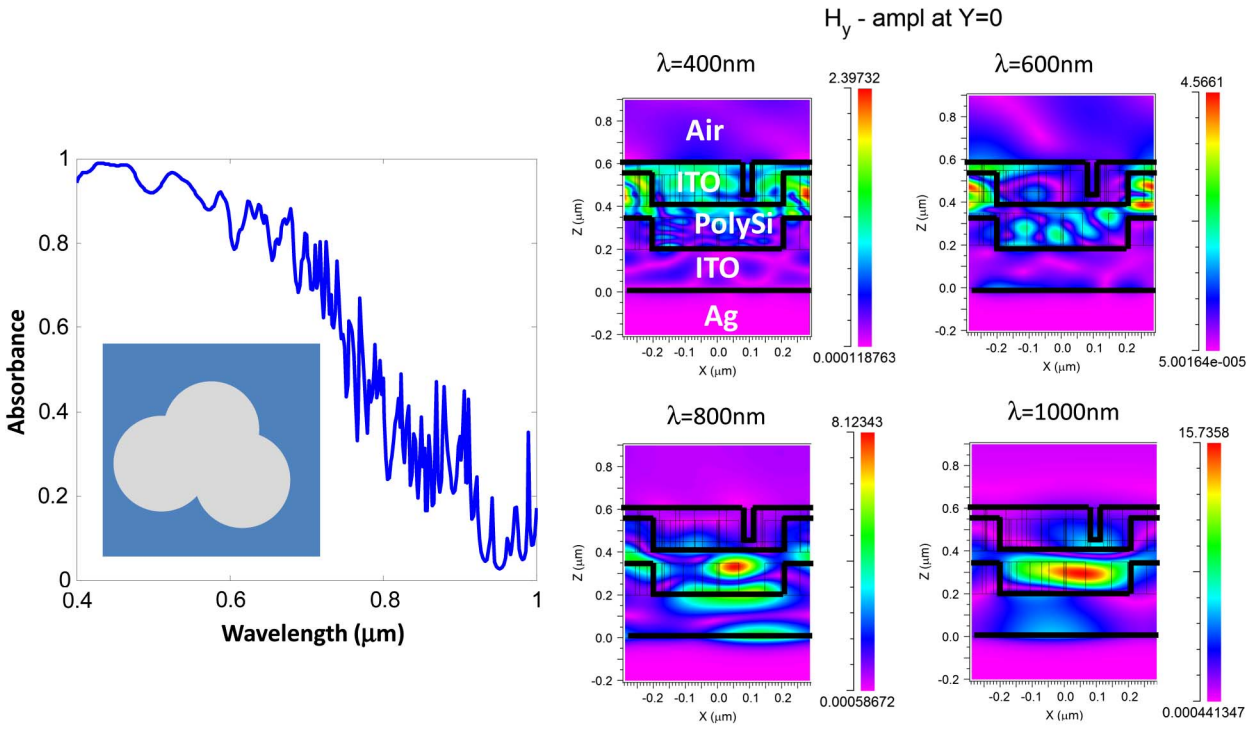

Fig. 5. (Left) Spectral absorbance for the pattern-designed, optimized structure; (right) the corresponding field profiles at 45-degree polarization incidence.

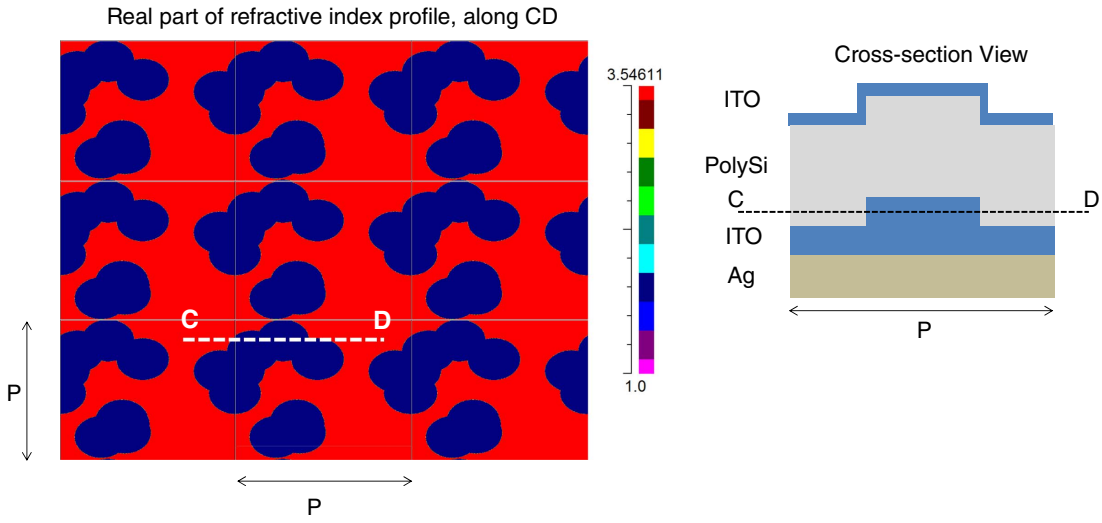

Fig. 6. Refractive index profile along the cross section CD, for the pattern-designed, optimized structure.

trapping. It has been clear from the literature [24] that, to boost the short circuit current (J_{SC}) in solar cells, the mode excitations should be designed carefully. There are actually three key factors affecting solar cell light trapping: resonance strength or equivalently mode confinement, mode quality factor, and the number of excited modes. Strong resonances may lead to only narrowband enhancement as can be seen in the baseline device in Section 3. Therefore, compromise between mode confinement, mode quality factor, and the number of quasi-guide modes is critical for a broadband slow-light enhancement.

The properly tailored geometry is the key to attaining the optimal trade-off between the three key factors mentioned above. This is because the photonic band structure ω-k is effectively tailored by the shape-optimized pattern. This is not surprising since it has been shown in the literature that the shape optimization can increase the photonic bandgap (PBG) [32]. Because more quasi-guided modes are excited in the pattern-design device, the slow-light enhancement is now covering a wider spectral range by a tailored ω-k, at some expense of increased photon group velocity (v_g) at the central resonance wavelength. Although v_g is slightly increased at the central resonance wavelength for the shape-optimized pattern, the broadband enhancement is still significantly improved compared to the baseline in Section 3. By comparing the spectral response in Figs. 3 and 5, the resonant strength of the quasi-guide mode excitations in the shape-optimized case is reduced, but more modes are excited to cover a broader spectral range. As a result, a single strongly resonant mode is broken into several weakly resonant modes using pattern design. This is especially pronounced in the long wavelength regime in the spectrum. Figure 6 shows the refractive index profile to illustrate the photonic pattern after optimization.

5. CONCLUSION

Solar cell short circuit current is further boosted by more than 16% using complex photonic pattern design schemes, over a fully parameter-optimized circularly shaped grating. The proposal is extremely practical in semiconductor processing and widely applicable to all solar cell technologies, including silicon, CdTe, CIGS, and III-V compounds. Compared to regular periodic gratings, there is no need for grayscale or holographic lithography to realize such a shape-optimized periodic grating, and only one etching step is needed. Enhanced broadband absorption is attributed to the broadband slow-light enhancement and the optimal balance between guide mode strength, mode quality factor, and the number of mode excitations associated with the pattern-designed periodic grating. The number of quasi-guide modes is effectively increased to cover a broader spectral range as the result of the pattern-designed periodic grating. The underlying physics is that the photonic band structure ω-k is effectively tailored by the shape optimization. The photon group velocity (v_g) is therefore adjusted accordingly, to achieve a slow enhancement over a wider spectral range. The pronounced additional enhancement over the optimized baseline implies the potential of the pattern-designed gratings to beat the randomly textured isotropic Lambertian surface. In addition, a random surface is difficult to be optimized because of its overly large dimension.

Ministry of Science and Technology, Taiwan (MOST 103-2221-E-009 -066).

REFERENCES

1. V. Shah, H. Schade, M. Vanecek, J. Meier, E. Vallat-Sauvain, N. Wyrsch, U. Kroll, C. Droz, and J. Bailat, "Thin-film silicon solar cell technology," Prog. Photovoltaics Res. Appl. **12**, 113–142 (2004).
2. A. Shah, P. Torres, R. Tscharner, N. Wyrsch, and H. Keppner, "Photovoltaic technology: the case for thin-film solar cells," Science **285**, 692–698 (1999).
3. A. S. Lin, Y.-K. Zhong, S.-M. Fu, C.-W. Tseng, S.-Y. Lai, and W.-M. Lai, "Lithographically fabricable, optimized three-dimensional solar cell random structure," J. Opt. **15**, 105007 (2013).
4. X. Sheng, S. G. Johnson, J. Michel, and L. C. Kimerling, "Optimization-based design of surface textures for thin-film Si solar cells," Opt. Express **19**, A841–A850 (2011).
5. C. Lin and M. L. Povinelli, "Optimal design of aperiodic, vertical silicon nanowire structures for photovoltaics," Opt. Express **19**, A1148–A1154 (2011).

6. F. Pratesi, M. Burresi, F. Riboli, K. Vynck, and D. S. Wiersma, "Disordered photonic structures for light harvesting in solar cells," Opt. Express **21**, A460–A468 (2013).
7. E. R. Martins, J. Li, Y. Liu, V. Depauw, Z. Chen, J. Zhou, and T. F. Krauss, "Deterministic quasi-random nanostructures for photon control," Nat. Commun. **4**, 2665 (2013).
8. M. Burresi, F. Pratesi, K. Vynck, M. Prasciolu, M. Tormen, and D. S. Wiersma, "Two-dimensional disorder for broadband, omnidirectional and polarization-insensitive absorption," Opt. Express **21**, A268–A275 (2013).
9. K. Vynck, M. Burresi, and F. R. S. Wiersma, "Photon management in two-dimensional disordered media," Nat. Mater. **11**, 1017–1022 (2012).
10. A. Lin and J. D. Phillips, "Optimization of random diffraction gratings in thin-film solar cells using genetic algorithms," Sol. Energy Mat. Sol. **92**, 1689–1696 (2008).
11. W.-R. Wei, M.-L. Tsai, S.-T. Ho, S.-H. Tai, C.-R. Ho, S.-H. Tsai, C.-W. Liu, R.-J. Chung, and J.-H. He, "Above-11%-efficiency organic–inorganic hybrid solar cells with omnidirectional harvesting characteristics by employing hierarchical photon-trapping structures," Nano Lett. **13**, 3658–3663 (2013).
12. P. C. Tseng, M. A. Tsai, P. Yu, and H. C. Kuo, "Antireflection and light trapping of subwavelength surface structures formed by colloidal lithography on thin film solar cells," Prog. Photovoltaics Res. Appl. **20**, 135–142 (2012).
13. X. Sheng, S. G. Johnson, L. Z. Broderick, J. Michel, and L. C. Kimerling, "Integrated photonic structures for light trapping in thin-film Si solar cells," Appl. Phys. Lett. **100**, 111110 (2012).
14. Z. Yu and S. Fan, "Angular constraint on light-trapping absorption enhancement in solar cells," Appl. Phys. Lett. **98**, 011106 (2011).
15. W. E. I. Sha, W. C. H. Choy, and W. C. Chew, "Angular response of thin-film organic solar cells with periodic metal back nanostrips," Opt. Lett. **36**, 478–480 (2011).
16. U. W. Paetzold, E. Moulin, B. E. Pieters, R. Carius, and U. Rau, "Design of nanostructured plasmonic back contacts for thin-film silicon solar cells," Opt. Express **19**, A1219–A1230 (2011).
17. U. W. Paetzold, E. Moulin, D. Michaelis, W. Bottler, C. Wachter, V. Hagemann, M. Meier, R. Carius, and U. Rau, "Plasmonic reflection grating back contacts for microcrystalline silicon solar cells," Appl. Phys. Lett. **99**, 181105 (2011).
18. A. Naqavi, K. Söderström, F.-J. Haug, V. Paeder, T. Scharf, H. P. Herzig, and C. Ballif, "Understanding of photocurrent enhancement in real thin film solar cells: towards optimal one-dimensional gratings," Opt. Express **19**, 128–140 (2011).
19. S. A. Mann, R. R. Grote, J. Richard, M. Osgood, and J. A. Schuller, "Dielectric particle and void resonators for thin film solar cell textures," Opt. Express **19**, 25729–25740 (2011).
20. Z. Yu, A. Raman, and S. Fan, "Fundamental limit of nanophotonic light trapping in solar cells," Proc. Natl. Acad. Sci. USA **107**, 17491–17496 (2010).
21. Z. Yu, A. Raman, and S. Fan, "Fundamental limit of light trapping in grating structures," Opt. Express **18**, A366–A380 (2010).
22. K. Söderström, F.-J. Haug, J. Escarré, O. Cubero, and C. Ballif, "Photocurrent increase in n-i-p thin film silicon solar cells by guided mode excitation via grating coupler," Appl. Phys. Lett. **96**, 213508 (2010).
23. H. A. Atwater and A. Polman, "Plasmonics for improved photovoltaic devices," Nat. Mater. **9**, 205–213 (2010).
24. A. Lin, Y.-K. Zhong, and S.-M. Fu, "The effect of mode excitations on the absorption enhancement for silicon thin film solar cells," J. Appl. Phys. **114**, 233104 (2013).
25. C. Battaglia, C.-M. Hsu, K. S. Derstrom, J. Escarre, F.-J. Haug, M. Charriere, M. Boccard, M. Despeisse, D. T. L. Alexander, M. Cantoni, Y. Cui, and C. Ballif, "Light trapping in solar cells: can periodic beat random?" ACS Nano. **6**, 2790–2797 (2012).
26. V. Ganapati, O. D. Miller, and E. Yablonovitch, "Spontaneous symmetry breaking in the optimization of subwavelength solar cell textures for light trapping," in *38th IEEE Photovoltaic Specialist Conference* (IEEE, 2012), pp. 001572–001576.
27. C. Battaglia, J. Escarre, K. Soderstrom, L. Erni, L. Ding, G. Bugnon, A. Billet, M. Boccard, L. Barraud, S. D. Wolf, F.-J. Haug, M. Despeisse, and C. Ballif, "Nanoimprint Lithography for high-efficiency thin-film silicon solar cells," Nano Lett. **11**, 661–665 (2011).
28. Rsoft, *Rsoft CAD User Manual*, 8.2 ed. (Rsoft Design Group, 2010).
29. K.-H. Hung, T.-G. Chen, T.-T. Yang, P. Yu, C.-Y. Hong, Y.-R. Wu, and G.-C. Chi, "Antireflective scheme for InGaP/InGaAs/Ge triple junction solar cells based on TiO_2 biomimetic structures," in *IEEE Photovoltaic Specialists Conference* (IEEE, 2012), pp. 003322–003324.
30. A. Chipperfield, P. Fleming, H. Pohlheim, and C. Fonseca, *Genetic Algorithm Toolbox User Guide* (University of Sheffield, 1994).
31. B. Deken, S. Pekarek, and F. Dogan, "Minimization of field enhancement in multilayer capacitors," Comput. Mater. Sci. **37**, 401–409 (2006).
32. S. Preblea, M. Lipson, and H. Lipson, "Two-dimensional photonic crystals designed by evolutionary algorithms," Appl. Phys. Lett. **86**, 061111 (2005).
33. L. Shen, Z. Ye, and S. He, "Design of two-dimensional photonic crystals with large absolute band gaps using a genetic algorithm," Phys. Rev. B **68**, 035109 (2003).
34. H. Lipson and J. B. Pollack, "Automatic design and manufacture of robotic lifeforms," Nature **406**, 974–978 (2000).